

PAPER • OPEN ACCESS

Energy analysis of a hydrogen integrated system in the residential sector

To cite this article: Francesca Mennilli *et al* 2023 *J. Phys.: Conf. Ser.* **2648** 012057

View the [article online](#) for updates and enhancements.

You may also like

- [Performance Analysis of Hydrogen Fed Proton Conducting ITSOFC Cogeneration System](#)
Nizar Amir
- [Modelling and optimization of biomass-based cogeneration plant](#)
N.A.A Abdul Razak and Abdulhalim Abdulrazik
- [Cogeneration Plant Optimization](#)
N W Mitiukov, S V Spiridonov and G Z Samigullina

PRIME
PACIFIC RIM MEETING
ON ELECTROCHEMICAL
AND SOLID STATE SCIENCE

HONOLULU, HI
Oct 6-11, 2024

Abstract submission deadline:
April 12, 2024

Learn more and submit!

Joint Meeting of
The Electrochemical Society
•
The Electrochemical Society of Japan
•
Korea Electrochemical Society

Energy analysis of a hydrogen integrated system in the residential sector

Francesca Mennilli, Lingkang Jin, Mosè Rossi, Alice Mugnini, and Gabriele Comodi

Department of Industrial Engineering and Mathematical Sciences (DIISM), Università Politecnica Delle Marche, Ancona, Italy

f.mennilli@pm.univpm.it

Abstract. Nowadays, buildings are responsible for almost 40% of global energy consumption, which is addressed by thermal (e.g., heating, cooling, and hot water) and electric (e.g., lighting and household appliances) loads. To meet the residential energy demand and, at the same time, ensure the decarbonisation of the energy infrastructure, hydrogen-based cogeneration systems might represent a viable solution. This work aims at evaluating the performance of a green hydrogen integrated system consisting of a Proton Exchange Membrane (PEM) electrolyser, hydrogen storage tanks, and a PEM fuel cell to meet both the electricity and, partially, the thermal energy demands of a condominium located in the center of Italy. The analysis considers a single energy scenario in which a Photovoltaic (PV) plant installed on the roof is directly connected with the hydrogen integrated system without any withdrawal from the national grid (e.g., off-grid operation mode). Results showed that, during the year, the user is completely self-sufficient from the electricity demand point of view. Furthermore, 22% of the thermal need can be satisfied through the fuel cell cogeneration system.

1. Introduction

Global issues regarding climate change and greenhouse gas emissions are the most discussed international priorities so far. The 26th Glasgow Conference of the Parties (COP26) stressed the need to keep the global average temperature increase below +1.5°C [1]. Subsequently, the Sharm el-Sheikh COP27 confirmed the COP26 conclusions, also highlighting the urgent target of reaching carbon neutrality by 2050 [2]. In such a scenario, the penetration of Renewable Energy Sources (RESs) into the global energy sector is strictly required to meet the ever-increasing energy demand of end-users. Among the most contributors, the residential sector is responsible for almost 40% of global energy consumption. The European statistics state that households accounted for 27% of the final energy consumption in the EU in 2020 [3].

To meet the residential energy demand and, at the same time, ensure the decarbonisation of the energy infrastructure, hydrogen-based cogeneration systems might represent a viable solution; indeed, hydrogen produced with renewable sources, known as “green hydrogen”, can be used as energy vector to store energy for medium-long term periods as well as solve the variability issue of renewable sources that leads to grid instability. Maestre et al. [4] provided an analysis of standalone Renewable Hydrogen-



based Systems (RHSs) focusing on both the residential and building sectors. The analysed pilot plants reflected the possibility of achieving 100% energy self-sufficiency; however, the system is still not cost-competitive with current electricity grid prices, and economic incentives are needed to deploy this technology further. Lubello et al. [5] investigated the applicability of hydrogen systems and batteries in different geographical conditions in Italy. Their work highlighted how such systems are not economically competitive for a single dwelling, while another study from Jin et al. [6] demonstrated how hydrogen could be competitive from both the energy and the economic points of view when dealing with highly variable renewable sources such as small-scale hydropower.

However, to the authors' knowledge, an energy evaluation of stand-alone hydrogen systems in the residential sector has not been carried out yet where all the design phases, including the power calculation of the renewable source, are considered. This work aims at covering this research gap by evaluating the performance of a green hydrogen integrated system consisting of a PEM electrolyser, hydrogen storage tanks, and a PEM fuel cell to meet both the electricity and, partially, the thermal energy demands of a condominium located in Fano, center of Italy, by exploiting the available rooftop space for the PV plant. The analysis is performed considering a single energy scenario in which the PV plant is directly connected with the hydrogen integrated system without any withdrawal from the national grid (e.g., off-grid operation mode). In this case, the sizing of system components and energy production and consumption evaluations have been carried out to assess the energy self-sufficiency of such a system in the residential sector.

The paper is structured as follows: Section 2 describes the methodology used to design and model the system components. Section 3 describes the results by highlighting the main energy analysis outcomes. Finally, Section 4 reports the conclusions of the work and its future developments.

2. Methods

In this section, two semi-empirical models to model and resemble both the PEM electrolyser and the PEM fuel cell have been adopted and used for carrying on the energy analysis. The models have been then validated with experimental data available in the scientific literature; in particular, two datasets at three different temperatures have been used for both the electrolyser and the fuel cell model validation.

2.1. PEM electrolyser modelling and validation

The main performance curve of an electrolyser is the polarization one, which represents the relation between the current density and the cell voltage. This relation is expressed as follows:

$$V = N_c * (E_{OCV} + V_{act,a} + V_{act,c} + V_{ohm}) \quad (1)$$

where N_c is the number of electrolyser cells, E_{OCV} (V) is the open circuit voltage, $V_{act,a}$ (V) and $V_{act,c}$ (V) are the anode and cathode activation overpotential, respectively, and V_{ohm} (V) is the ohmic overpotential. The cell voltage is also affected by concentration losses that occur at high current densities. Indeed, the reaction rate is slowed down by the overpopulation of reacting molecules when dealing with high current densities. In PEM electrolysers, this behaviour is not observed until mild operating current densities are achieved (e.g., 1.6 A/cm²) [7]. For this reason, this value of current has

been chosen as the maximum limit of the model to have a good compromise between efficiency and hydrogen production. The open circuit voltage is determined using the Nernst's equation [7]:

$$E_{OCV} = E_{rev} + \frac{R*T}{n*F} * \ln \frac{P_{H2} * P_{O2}^{0.5}}{P_{H2O}} \quad (2)$$

where P (Pa) is the partial pressure of reactants/products, T (K) is the cell temperature, F (C/mol) is the Faraday's constant, R (J/mol*K) is the universal gas constant, and E_{rev} (V) is the reversible cell potential. The latter is calculated using the empirical expression [7]:

$$E_{rev} = 1.229 - 0.9 * 10^{-3} * (T - 298) \quad (3)$$

Regarding the calculation of partial pressures, it has been assumed that i) the liquid water circulating into the electrolyser exerts a partial pressure, which is equal to its saturated vapour pressure at a given temperature [8], and ii) both the anode and the cathode operate at atmospheric pressure.

Regarding the activation overpotential calculation, a simplified expression based on the Butler-Volmer's equation, which is the so-called Tafel's equation, is used for both anode and cathode [7]:

$$V_{act,x} = \frac{R*T}{n*F*\alpha_x} * \ln \left(\frac{i}{i_{0,x}} \right) \quad (4)$$

where α_x is the charge transfer coefficient of the anode and the cathode [9], i (A/cm²) is the current density, and $i_{0,x}$ (A/cm²) is the exchange current density of the anode and the cathode. The latter is calculated with the Arrhenius' equation [10] by knowing the reference exchange current density of the anode and the cathode $i_{0x,ref}$ (A/cm²) [11] and their activation energy $E_{act,x}$ (J/mol) [10, 12] as well. Ohmic losses are evaluated with the Ohm's law, which is commonly used to consider the membrane resistance, but it can also be applied to both diffusion and catalytic layers [7]. The equation is the following:

$$V_{ohm} = \frac{\delta}{\sigma} * i \quad (5)$$

where δ (m) is the membrane thickness and σ (S/m) is the membrane conductivity. The latter is calculated with the Arrhenius' equation by knowing the membrane reference conductivity σ_{ref} (S/m) [13] and the proton membrane activation energy E_{pro} (J/mol) [14]. The rate of produced hydrogen is evaluated with the Faraday's law [9] as follows:

$$\dot{n}_{H2} = \frac{\eta_f * i * A_{cell} * N_c}{2 * F} \quad (6)$$

where A_{cell} (m²) is the cell area and η_f is the Faraday's efficiency that is assumed equal to 100% according to [9]. The electric power consumption is evaluated as follows:

$$P_{el} = V * i * A_{cell} * N_c \quad (7)$$

and, finally, the energy efficiency (electricity conversion into hydrogen) is given by:

$$\eta = \frac{P_{out}}{P_{in}} = \frac{\dot{m} * H_2 * LHV}{P_{el}} \quad (8)$$

The PEM electrolyser model validation has been performed using experimental data of [15]. The validation referred to 60°C, 70°C, and 80°C since these temperatures represent the typical operating range of this kind of technology [11]. As shown in Figure 1, the proposed model provides a good fit between simulated and real data, although there is a deviation of the experimental points from the model in the activation zone. This behavior is mainly due to differences in i) electrode materials and their catalysts, which affect the activation energy and the exchange current density, and ii) different membrane materials that affect the charge transfer coefficient and the proton activation energy. However, the calculation of the Root Mean Square Errors (RMSEs) reported in Figure 1, whose range goes from 0.019 V to 0.068 V, confirms the reliability of the proposed model.

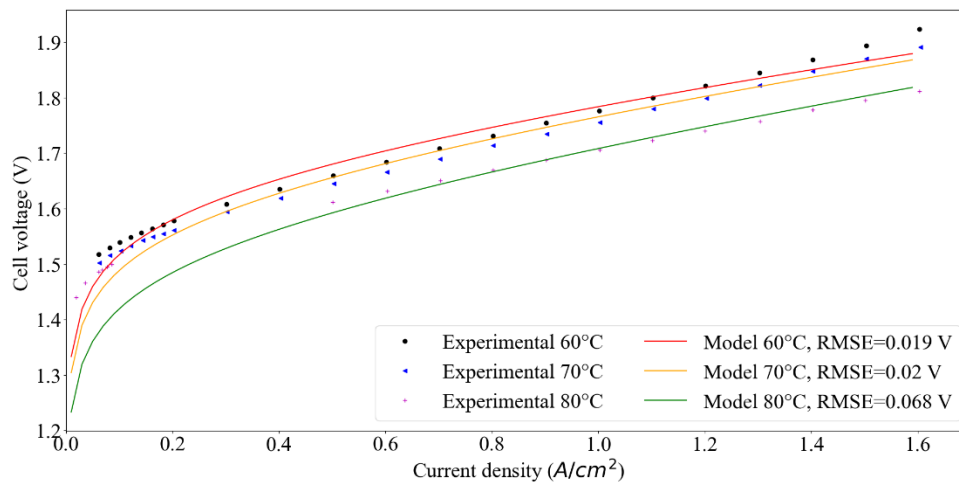


Figure 1 – PEM electrolyser model validation.

2.2. PEM fuel cell modelling and validation

Similarly, the main representation of the PEM fuel cell performance is the polarization curve, which is expressed as:

$$V = N_c * (E_{OCV} - V_{act,a} - V_{act,c} - V_{ohm} - V_{conc}) \quad (9)$$

where V_{conc} (V) is the concentration overpotential. The open circuit voltage is calculated with the same equation as for the electrolyser (see Eq. 2), where E_{rev} (V) is obtained by knowing the entropy and enthalpy change as a function of the temperature [16]. Partial pressures of reactants, if they are pure, are considered equal to the fuel cell inlet pressure. If there is air instead of oxygen at the cathode, the oxygen partial pressure will be equal to 21% of the inlet pressure according to the air chemical composition. The partial pressure of water is equal to 1 bar when the product of the reaction is liquid water [17]. Regarding the activation overpotential calculation, the same approach used for the electrolyser is applied (see Eq. 4) once α_x [18], $i_{0x,ref}$ (A/cm²) [16, 19], and $E_{act,x}$ (J/mol) [19] are determined. Ohmic losses are evaluated as follows:

$$V_{ohm} = i * A_{cell} * (R_{mem} + R_c) \quad (10)$$

where A_{cell} (m^2) is the cell area, R_{mem} (Ω) is the fuel cell electrode electronic resistance [20], and R_c (Ω) is the membrane ionic resistance [19]. Concentration losses are calculated as follows:

$$V_{conc} = \frac{R*T}{n*F} * \ln \frac{i_{max}}{i_{max}-i} \quad (11)$$

where i_{max} (A/cm^2) is the limit current density, namely the one generated when the reactants concentration is equal to zero that means that they are instantly consumed in the electrochemical cell [16]. The electric power production is evaluated through Eq. 7, while the thermal power production is written as:

$$P_{th} = i * A_{cell} * N_c * (V_{H2} - V) \quad (12)$$

where V_{H2} (V) is the equivalent voltage corresponding to the Higher Heating Value (HHV) of hydrogen [16]. Finally, the PEM fuel cell energy efficiency is given by Eq. 13:

$$\eta = \frac{P_{out}}{P_{in}} = \frac{P_{el}}{\dot{m}_{H2} * HHV} \quad (13)$$

while hydrogen consumption can be evaluated through the Faraday's law [16]:

$$\dot{n}_{H2} = \frac{i * A_{cell} * N_c}{2 * F} \quad (14)$$

The PEM fuel cell model validation has been performed using experimental data of [21]. Experimental data of PEM fuel cells operating at 50, 60, and 70°C have been used since these temperatures represent the typical operating range of this type of technology [16]. As shown in Figure 2, the proposed model provides a good agreement with real data. This result is also confirmed by RMSEs values, whose range goes from 0.0154 V to 0.0159 V that makes the model reliable as much as the electrolyser one.

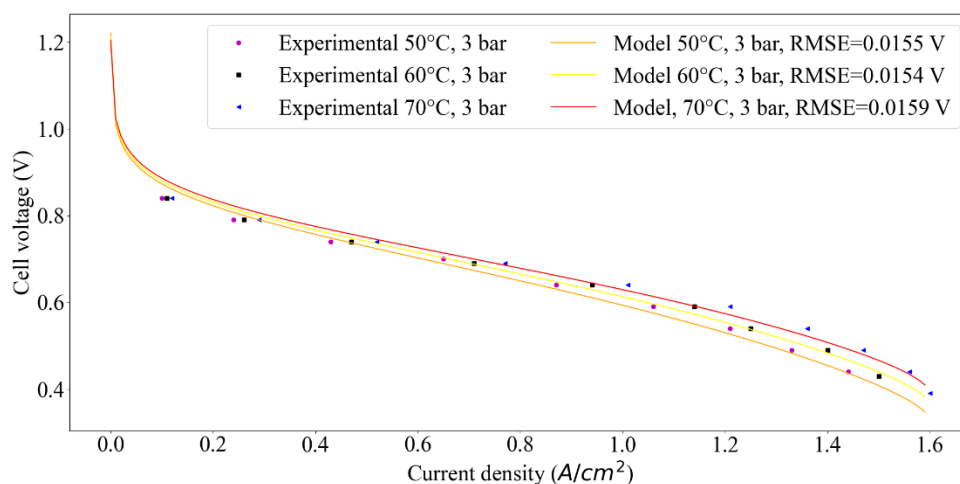


Figure 2 – PEM fuel cell model validation.

2.3. PV plant and hydrogen system design

This work is focused on the energy analysis of a condominium located in Fano, centre of Italy, when it is directly connected with a hydrogen integrated system powered by a PV plant installed on the roof. In this case, both the roof surface exposition and the available area have been analysed and calculated to evaluate the maximum capacity of the PV plant. All the technical parameters referred to the latter are listed in Table 1.

The PEM electrolyser design has been performed considering the number of occurrences for the electric power input from the PV plant. In particular, it was found that most of the produced electric powers lies in the range 0-3 kW, even though the PV plant production range goes from 0 to 15 kW. However, since the hydrogen production corresponding to this electric power range is low, it has been decided to cut the electric power below 3 kW to exploit the higher power rating from the PV plant, which allows to produce more hydrogen. The PEM fuel cell design has been performed considering the electric load to be satisfied.

Table 1 – Technical parameters of the PV plant.

	Roof exposition: S-E	Roof exposition: N-W
Available surface (m²)	104	82
Occupied surface (m²)	70.56	54.6
DC-DC converter (V)	220	220
Output current (A)	44	29.32
Rated power (kW)	15	12

3. Results and comments coming from a case study

In this section, the PV plant production and the PEM electrolyser consumption and PEM fuel cell production are discussed together with their hydrogen flow rate production and consumption, respectively.

The yearly PV production has been calculated (e.g., hourly resolution) and reported in Figure 3: these data are related to the technical characteristics of the PV plant reported in Table 1. The energy production profile has a peak of 15.77 kW at 11 am on May 28th.

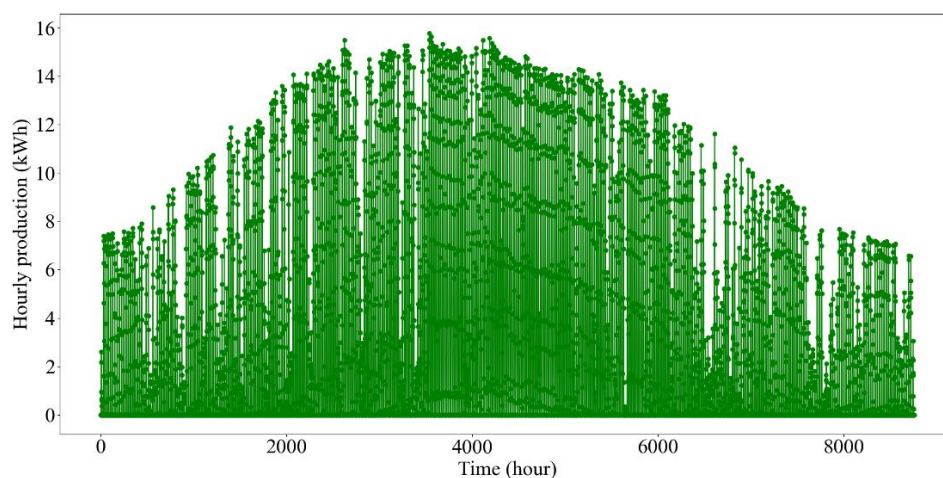


Figure 3 – PV plant hourly production during the year (8,760 h).

The daily electricity consumption profile (e.g., hourly basis) of the building has been assumed according to [22]. Starting from the average daily electricity consumption profile of an Italian family with four persons, the hourly electricity demand has been obtained based on the overall electricity consumption of the building under investigation. However, due to the lack of data, this profile has been repeated all over the year. The peak power is 3.38 kW and the total electricity demand in the year is 13,362 kWh.

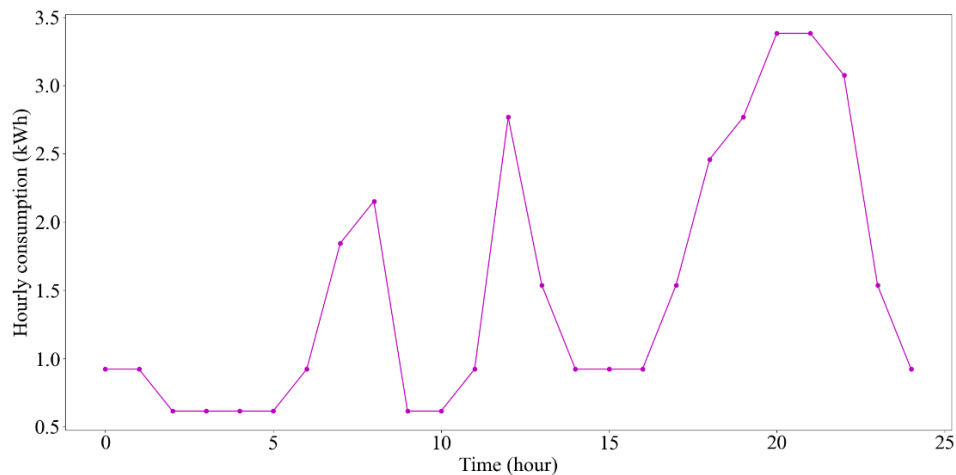


Figure 4 – Daily electricity consumption profile.

The energy analysis of the hydrogen integrated system allowed to establish the quantity of excess electric energy flowing into the electrolyser and used to produce hydrogen, as well as the quantity of electric energy that must be produced by the fuel cell. In particular, 21,062 kWh are used throughout the year to produce hydrogen, while 8,290 kWh must be generated by the PEM fuel cell. It is worth noting that, in the case of only PV production without the hydrogen integrated system, the electric energy produced by the PEM fuel cell must be withdrawn from the national grid.

Both the PEM electrolyser and the PEM fuel cell have been sized based on energy flow results. It is worth noting that values of the number of cells and cell area (m^2), which come from calculations, are within the ranges provided by [23, 24].

Table 2 – PEM electrolyser and PEM fuel cell characteristics.

	PEM electrolyser	PEM fuel cell
Rated power (kW)	13	3
Number of cells	200	200
Cell area (cm^2)	42.6	25
Hydrogen flow rate (Nm^3/h)	5.66	2.83
Electric efficiency range	0.67-0.76	0.42-0.77
Current density (A/cm^2)	0.4-1.6	0-1.35
Cell potential (V)	1.65-1.88	0.5-0.9

As it can be noticed, the electrolyser has been slightly oversized to always meet the energy demand; indeed, the yearly hydrogen production is $7,095 \text{ Nm}^3$, while the yearly hydrogen consumption is $6,902 \text{ Nm}^3$. As a result, there is an annual excess of hydrogen equal to 2.7% of the total production of hydrogen

by the electrolyser. This excess is stored in hydrogen storage tanks. The energy excess from the PV plant is directly sent to the electrolyser to produce hydrogen. The yearly hydrogen production is strictly connected to the PEM fuel cell operation since this technology will supply the electricity demand of the condominium completely. That said, knowing the electricity profile that the fuel cell must supply to the condominium, the highest hydrogen volume needed to fully cover the worst day of the year from an energy point of view must be calculated. Finally, it has been obtained that August 24th is the worst day as shown in Figure 5, where the difference between energy production and consumption is always lower than 0. This means that it will be necessary to use the hydrogen stored in the previous days to satisfy the electricity demand; thus, it must be verified that a proper quantity of hydrogen is stored. It has been verified that, starting from 22nd August, the amount of hydrogen stored in proper tanks to be sent to the PEM fuel cell can satisfy the electricity demand of the condominium on August 24th, as well as in the next days of the year. This means that, during the year, the hydrogen produced is always sufficient to cover the electricity demand of the condominium through the PEM fuel cell. End-users can therefore be energetically independent with the integrated hydrogen system. Furthermore, the thermal power demand for heating and for hot water (73,251 kW_{th}) is partially covered by the PEM fuel cell heat production (cogeneration mode): indeed, 22% of the thermal power need during the year by the condominium is satisfied.

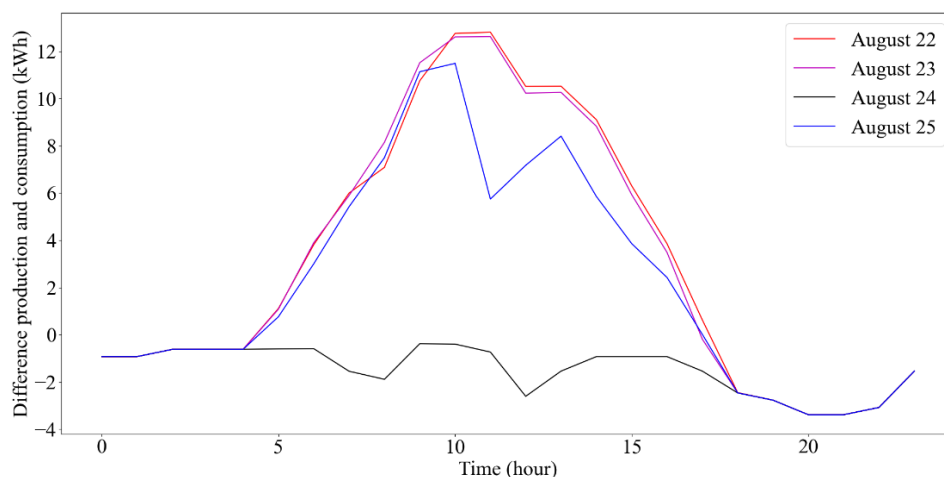


Figure 5 – Difference between PV plant production and consumption in August 22nd, 23rd, 24th, and 25th.

4. Conclusions

The present work has the aim to evaluate the feasibility of a hydrogen integrated system applied in the residential sector from an energy point of view. Considering a condominium located in the center of Italy, a PV plant installed on the roof is directly connected with the hydrogen integrated system without any withdrawal from the national grid (e.g., off-grid operation mode). The electrolyser has been slightly oversized to always meet the energy demand; thus, there is an annual excess of hydrogen equal to 2.7% of the total production of the PEM electrolyser, which is stored in hydrogen storage tanks. It has also been verified that, during the worst energetically day of the year (e.g., August 24th), the electricity demand is completely covered by the PEM fuel cell. This means that, during the year, the electricity

demand is satisfied by the PEM fuel cell, thus guaranteeing the independency of the end-users. Furthermore, if the PEM fuel cell operates in cogeneration mode, it is possible to supply 22% of the total thermal power required by the condominium. Finally, the energy analysis gave positive results, demonstrating that the application of a hydrogen integrated system without any other equipment for energy storage (e.g., electric batteries) is energetically feasible in the residential sector. Future studies will be devoted to the optimization of the hydrogen integrated system size, as well as distinguishing thermal energy demand in heating and hot water ones for the proper assessment of the thermal energy demand fulfilled by the PEM fuel cell. Then, an economic analysis of the overall system will be also investigated.

References

- [1] Low, M., & Rai, S. C. *Key Outcomes of COP26: The Glasgow Climate Pact*.
- [2] Kedia, S., Cholayil, N., Mathur, A., Banerjee, S., Goel, S., Das, S., & Rashmi, R. Act4Earth COP27 compass policy brief road to Sharm El-Sheikh: Towards equity and climate justice authors acknowledgments.
- [3] Eurostat, (June 17th, 2022). Energy use in households in 2020. <https://ec.europa.eu/eurostat/en/web/main/home> (last accessed on May 23rd, 2023).
- [4] Maestre, V. M., Ortiz, A., & Ortiz, I. (2022). The role of hydrogen-based power systems in the energy transition of the residential sector. In *Journal of Chemical Technology and Biotechnology* (Vol. 97, Issue 3, pp. 561–574). John Wiley and Sons Ltd. <https://doi.org/10.1002/jctb.6938>.
- [5] Lubello, P., Pasqui, M., Mati, A., & Carcasci, C. (2022). Assessment of hydrogen-based long term electrical energy storage in residential energy systems. *Smart Energy*, 8. <https://doi.org/10.1016/j.segy.2022.100088>.
- [6] Jin, L., Rossi, M., Monforti Ferrario, A., Alberizzi, J. C., Renzi, M., & Comodi, G. (2023). Integration of battery and hydrogen energy storage systems with small-scale hydropower plants in off-grid local energy communities. *Energy Conversion and Management*, 286. <https://doi.org/10.1016/j.enconman.2023.117019>.
- [7] Falcão, D. S., & Pinto, A. M. F. R. (2020). A review on PEM electrolyzer modelling: Guidelines for beginners. In *Journal of Cleaner Production* (Vol. 261). Elsevier Ltd. <https://doi.org/10.1016/j.jclepro.2020.121184>.
- [8] Biaku, C. Y., Dale, N. V., Mann, M. D., Salehfar, H., Peters, A. J., & Han, T. (2008). A semiempirical study of the temperature dependence of the anode charge transfer coefficient of a 6 kW PEM electrolyzer. *International Journal of Hydrogen Energy*, 33(16), 4247–4254. <https://doi.org/10.1016/j.ijhydene.2008.06.006>.
- [9] Tijani, A. S., Binti Kamarudin, N. A., & Binti Mazlan, F. A. (2018). Investigation of the effect of charge transfer coefficient (CTC) on the operating voltage of polymer electrolyte membrane (PEM) electrolyzer. *International Journal of Hydrogen Energy*, 43(19), 9119–9132. <https://doi.org/10.1016/j.ijhydene.2018.03.111>.
- [10] Kaya, M. F., & Demir, N. (2017). Numerical Investigation of PEM Water Electrolysis Performance for Different Oxygen Evolution Electrocatalysts. *Fuel Cells*, 17(1), 37–47. <https://doi.org/10.1002/fuce.201600216>.

- [11] Carmo, M., Fritz, D. L., Mergel, J., & Stolten, D. (2013). A comprehensive review on PEM water electrolysis. In *International Journal of Hydrogen Energy* (Vol. 38, Issue 12, pp. 4901–4934). <https://doi.org/10.1016/j.ijhydene.2013.01.151>.
- [12] He, Z. Da, Wei, J., Chen, Y. X., Santos, E., & Schmickler, W. (2017). Hydrogen evolution at Pt(111) – activation energy, frequency factor and hydrogen repulsion. *Electrochimica Acta*, 255, 391–395. <https://doi.org/10.1016/j.electacta.2017.09.127>.
- [13] García-Valverde, R., Miguel, C., Martínez-Béjar, R., & Urbina, A. (2008). Optimized photovoltaic generator-water electrolyser coupling through a controlled DC-DC converter. *International Journal of Hydrogen Energy*, 33(20), 5352–5362. <https://doi.org/10.1016/j.ijhydene.2008.06.015>.
- [14] Ito, H., Maeda, T., Nakano, A., & Takenaka, H. (2011). Properties of Nafion membranes under PEM water electrolysis conditions. In *International Journal of Hydrogen Energy* (Vol. 36, Issue 17, pp. 10527–10540). <https://doi.org/10.1016/j.ijhydene.2011.05.127>.
- [15] García-Valverde, R., Espinosa, N., & Urbina, A. (2012). Simple PEM water electrolyser model and experimental validation. *International Journal of Hydrogen Energy*, 37(2), 1927–1938. <https://doi.org/10.1016/j.ijhydene.2011.09.027>.
- [16] Barbir, F. (2013). *PEM fuel cells, theory and practice* (2nd ed.). Elsevier.
- [17] Larminie, James., & Dicks, Andrew. (2003). *Fuel cell systems explained*. J. Wiley.
- [18] Song, C., Tang, Y., Zhang, J. L., Zhang, J., Wang, H., Shen, J., McDermid, S., Li, J., & Kozak, P. (2007). PEM fuel cell reaction kinetics in the temperature range of 23-120 °C. *Electrochimica Acta*, 52(7), 2552–2561. <https://doi.org/10.1016/j.electacta.2006.09.008>.
- [19] Rahman, M. A., Mojica, F., Sarker, M., & Chuang, P. Y. A. (2019). Development of 1-D Multiphysics PEMFC model with dry limiting current experimental validation. *Electrochimica Acta*, 320. <https://doi.org/10.1016/j.electacta.2019.134601>.
- [20] Živko, D., & Bilas, V. (n.d.). *Analysis of individual PEM fuel cell operating parameters for design of optimal measurement and control instrumentation*.
- [21] Wang, L., Husar, A., Zhou, T., & Liu, H. (2003). A parametric study of PEM fuel cell performances. *International Journal of Hydrogen Energy*, 28(11), 1263–1272. [https://doi.org/10.1016/S0360-3199\(02\)00284-7](https://doi.org/10.1016/S0360-3199(02)00284-7).
- [22] Fotovoltaico e batterie su abitazione - l'esempio tipico di abitazione in Italia (Oct. 7th, 2014). <https://www.energyhunters.it/fotovoltaico-e-batterie-su-abitazione-lesempio-tipico-di-abitazione-in-italia/> (last accessed on May 23rd, 2023).
- [23] Chang, H., Xu, X., Shen, J., Shu, S., & Tu, Z. (2019). Performance analysis of a micro-combined heating and power system with PEM fuel cell as a prime mover for a typical household in North China. *International Journal of Hydrogen Energy*, 44(45), 24965–24976. <https://doi.org/10.1016/j.ijhydene.2019.07.183>.
- [24] Sinha, R. (Jan. 10, 2022). The critical role of materials in the high price of PEM electrolyzers. <https://www.newtrace.io/product> (last accessed on May 23rd, 2023).